MEASUREMENT OF D_s^\pm AND CABIBBO-SUPPRESSED D^\pm DECAYS

M.P. Alvarez², R. Barate^{3b}, D. Bloch⁹, P. Bonamy⁷, P. Borgeaud⁷,
M. Burchell⁴, H. Burmeister³, J.M. Brunet⁶, F. Calvino^{2a}, M. Cattaneo⁴,
J.M. Crespo², B. d'Almagne⁵, M. David⁷, L. DiCiaccio^{3c}, J. Dixon⁴, P. Druet⁵,
A. Duane⁴, J.P. Engel⁹, A. Ferrer^{3d}, T.A. Filippas¹, E. Fokitis¹, R.W. Forty⁴,
P. Foucault⁹, E.N. Gazis¹, J.P. Gerber⁹, Y. Giomataris³, T. Hofmokl¹⁰,
E.C. Katsoufis¹, M. Koratzinos^{3,4,5}, C. Krafft⁵, B. Lefievre⁶, Y. Lemoigne⁷,
A. Lopez^{3,5*}, W.K. Lui⁸, C. Magneville⁷, A. Maltezos¹, J.G. McEwen⁸,
Th. Papadopoulou¹, B. Pattison³, D. Poutot⁶, M. Primout⁷, H. Rahmani¹,
P. Roudeau⁵, C. Seez⁴, J. Six⁵, R. Strub⁹, D. Treille³,
P. Triscos⁶, G. Tristram⁶, G. Villet⁷, A. Volte⁶, M. Wayne⁵,
D.M. Websdale⁴, G. Wormser⁵ and Y. Zolnierowski³

(The NA14/2 Collaboration)

(Submitted to Physics Letters)

-
- 1) National Technical University, Athens, Greece.
 - 2) Universidad Autónoma de Barcelona, Bellaterra, Spain.
 - 3) CERN, Geneva, Switzerland.
 - 4) Blackett Lab., Imperial College, London, UK.
 - 5) LAL, IN2P3-CNRS and Univ. Paris-Sud, Orsay, France.
 - 6) Collège de France, Paris, France.
 - 7) DPhPE, CEN-Saclay, Gif-sur-Yvette, France.
 - 8) Univ. of Southampton, Southampton, UK.
 - 9) CRN, IN2P3-CNRS and Univ. L. Pasteur, Strasbourg, France.
 - 10) Univ. of Warsaw, Warsaw, Poland.
 - a) Univ. Politecnica de Catalunya, ETSEIB-DEN, Barcelona, Spain.
 - b) Univ. J. Fourier and ISN, Grenoble, France.
 - c) Univ. di Roma II, 'Tor Vergata', Rome, Italy.
 - d) Univ. de Valencia, IFIC, Valencia, Spain.
 - *) On leave from Fac. de Ciencias Fisicas, Univ. Complutense, Madrid, Spain.

ABSTRACT

The CERN charm photoproduction experiment NA14/2 has studied the $K^+K^-\pi^+$, $\phi\pi^+$, $\phi\pi^+\pi^0$, and $\phi\pi^+\pi^+\pi^-$ decay modes of the D_s^+ and D^+ charmed mesons, and the corresponding charge conjugate states. We measure branching ratios:

$$\text{Br}(D^+ \rightarrow \phi\pi^+)/\text{Br}(D^+ \rightarrow K^-\pi^+\pi^+) = 0.098 \pm 0.032 \pm 0.014$$

$$\text{Br}(D_s^+ \rightarrow \bar{K}^{*0}K^+)/\text{Br}(D_s^+ \rightarrow \phi\pi^+) = 0.85 \pm 0.34 \pm 0.20$$

and obtain upper limits for the other channels. Contrary to the prediction of some theoretical models, we do not observe any decay of D_s into $\phi\rho$. Using the Lund Monte Carlo to hadronize the final-state partons we derive a value for the absolute branching fraction $\text{Br}(D_s^+ \rightarrow \phi\pi^+) = 4.8 \pm 1.7 \pm 1.9\%$.

1. INTRODUCTION

In photoproduction the yield of charmed particles per hadronic event is about ten times higher than that from incident hadrons. This is because photons couple directly with the quarks in the nucleon target, leading to a higher effective centre-of-mass energy available for the creation of heavy quarks. This feature is useful in a study of D_s^+ decays and of Cabibbo-suppressed D^+ decays ^{*)}.

The experiment described here used the NA14 spectrometer [1]. As the photoproduction rate of charmed particles is two orders of magnitude lower than the total hadronic rate, a high-precision vertex detector has been added to the spectrometer [2]. It consists of a silicon active target and 10 planes of 50 μm pitch microstrips, and is used to identify short-lived decays. Spatial reconstruction of the production and decay vertices is achieved in the microstrips with a 15 μm (300 μm) precision in the transverse (longitudinal) direction with respect to the beam. The active target consists of 32 planes each segmented into strips at 2.1 mm pitch. The level of ionization that is measured close to the decay vertex allows identification and rejection of reinteracting secondaries.

Charged particles, with momenta measured in the spectrometer, are identified using an air-filled Cherenkov counter. The threshold condition allows the separation of kaons/protons from pions between 6.3 and 20.5 GeV/c and protons from kaons/pions above 21 GeV/c.

During the period 1985–86 a total of 17 million events were recorded. The trigger condition required a hadronic interaction in the target leading to at least one charged particle above and one below the horizontal plane containing the beam axis.

High-statistics samples of reconstructed D^0 and D^+ decays were obtained in various decay channels. Lifetimes were measured, and photoproduction of charmed particles has been studied [3, 4]. The gross features of weak decays of charmed particles can be understood as the β -decay of the charmed quark, independent of the presence of other quarks in the hadron. This simple spectator model is complicated by gluon corrections, interference, and final-state interactions. There are also contributions to the decay which are not of the spectator type (annihilation, exchange, ...) [5]. The importance of these effects is demonstrated by the large lifetime difference observed between the various charmed particles. It is hoped that by studying several decay modes the contribution from the different decay mechanisms can be determined.

This paper presents our results on D^+ and D_s^+ decays involving two charged kaons in the final state.

2. DATA PROCESSING

The data were passed, in parallel, through two independent filter algorithms.

One filter performed a fast track reconstruction using the multiwire proportional chambers (MWPCs) to calculate approximate momenta, and the Cherenkov counter selected events containing two (or more) kaons. The efficiency of this filter is about 75% [6, 7].

The other filter used the information from the vertex detector to select events with tracks offset from the production vertex. This resulted in a sample of events enriched with charmed-particle decays. The filter retained 18% of the events, while the efficiency for events with charmed-particle decays was measured to be about 60% [8].

^{*)} Throughout the paper, the charge-conjugate states are implicitly included.

Both filtered samples were then processed through a full pattern-recognition and track-reconstruction program, which uses coordinates measured in the MWPC and microstrips. The vertex analysis was performed as follows. A decay vertex was reconstructed using the appropriate combination of tracks for a given decay channel. The production vertex was reconstructed using the resultant of the momentum vectors at the decay vertex, together with all other charged tracks in the event. Tracks contributing with bad χ^2 to the vertex are dropped and the process iterated until a good overall χ^2 probability is obtained. This procedure permits the elimination from the fit of tracks from the decay of the accompanying charmed particle. For each event all acceptable assignments of tracks to vertices are retained.

The charmed-particle signals are then extracted by imposing a cut on the vertex separation distance along the beam direction Δx , or on this distance, scaled by its error σ_x (determined from the errors on production and decay vertices), $N_\sigma = \Delta x / \sigma_x$.

3. SPECTROSCOPY OF D_s^+ AND D^+ PARTICLES WITH TWO CHARGED KAONS IN THE FINAL STATE

The $\phi\pi^+$ decay channel is shown in fig. 1, with data from both filtered samples combined. A clear signal is seen for the decay $D_s^+ \rightarrow \phi\pi^+$, and also for the Cabibbo-suppressed D^+ decay into the same final state. Each decay channel studied in this paper has been simulated using a Monte Carlo method that incorporates the properties of the detectors and uses the same reconstruction algorithms as are used on the real data. The charm photoproduction is generated using the photon-gluon fusion model and the final-state partons are hadronized using the Lund model. Good agreement has been found for production kinematic variables between real and Monte Carlo data, both for the D_s and for the high-statistics D^0 sample [4, 7]. Reconstruction efficiencies appropriate for a given decay channel have been extracted. For the D^+ we have normalized the various decay channels to the $K^-\pi^+\pi^+$ final state and for the D_s^+ we have used the $\phi\pi^+$ as reference.

3.1 The $K^+K^-\pi^+$ final state

We extract the ratio $\text{Br}(D^+ \rightarrow \phi\pi^+)/\text{Br}(D^+ \rightarrow K^-\pi^+\pi^+)$. To minimize systematic uncertainties, the same vertex separation cuts were applied to the two channels. These retained 341 ± 28 decays in the $K^-\pi^+\pi^+$ and 12 ± 4 decays in the $\phi\pi^+$ channels. The result, given in Table 1, assumes a value for the branching fraction $\text{Br}(\phi \rightarrow K^+K^-) = 0.495$. The systematic error is mainly due to the uncertainty in acceptance of the detector for the two kaons, which have different energy spectra in the two decay modes.

Figure 2 shows the mass distribution for the channel $\bar{K}^{*0}K^+$, where a signal of 9 ± 3 events is seen for the D_s^+ . Even with harder cuts on the decay lengths to reduce the background, no evidence for a D^+ decay has been found in this channel [6, 8].

Tables 1 and 2 summarize these results. They show, as already observed in the comparison of D^0 decay into $K^-\pi^+$ and $\bar{K}^0\pi^0$ [9], that the so-called ‘colour suppression mechanism’ does not operate. From this mechanism we would have expected a large enhancement for the decay $D^+ \rightarrow \bar{K}^{*0}K^+$ relative to $D^+ \rightarrow \phi\pi^+$ and also for $D_s^+ \rightarrow \phi\pi^+$ relative to $D_s^+ \rightarrow \bar{K}^{*0}K^+$.

3.2 The $\phi\pi^+\pi^0$ final state

We have searched for signals in the $\phi\pi^+\pi^0$ decay mode. In this analysis, the two photons from the π^0 are measured in the forward electromagnetic calorimeter.

Confidence in our ability to measure final states involving photons is provided by our observation [4] of the well-established $K^-\pi^+\pi^0$ decay mode of the D^0 meson.

We measure the photon-detection efficiency ε_γ of the electromagnetic calorimeter using two independent methods. In the first method we assume, from isospin considerations, that the number of π^0 's photoproduced is half the number of π^\pm . By changing a π^\pm in the raw data into a π^0 we can then simulate the two-photon decay and thus calculate the value ε_γ for our detectors. The second method uses an analysis of clusters in the calorimeter data. We measure $\varepsilon_\gamma = 0.52$ and $\varepsilon_\gamma = 0.49$ respectively using the two methods. We adopt the value $\varepsilon_\gamma = 0.50 \pm 0.03$ and find $\text{Br}(D^0 \rightarrow K^-\pi^+\pi^0)/\text{Br}(D^0 \rightarrow K^-\pi^+) = 4.0 \pm 0.9 \pm 1.0$, which is compatible with published data [10].

Figure 3 shows the $\phi\pi^+\pi^0$ mass distribution with a vertex cut $N_\sigma > 8$. No events are seen in the D_s^+ region and the upper limit for the branching ratio is given in Table 2. The three events in the D^+ region disappear when we apply a stronger cut and the corresponding limit is given in Table 1.

The upper limit for $\text{Br}(D_s^+ \rightarrow \phi\pi^+\pi^0)/\text{Br}(D_s^+ \rightarrow \phi\pi^+) < 2.6$ at 90% confidence level (CL) was calculated assuming a D_s^+ decay according to phase space. The effect on the acceptance of a possible $\phi\rho^+$ mode is small (about 10%). Our measured limit is therefore in disagreement with the predicted ratio of 6.3 [11]. For the same channel the E691 Collaboration measured a value [12] that is compatible with our limit.

3.3 The $\phi\pi^+\pi^+\pi^-$ final state

We have investigated the $\phi\pi^+\pi^+\pi^-$ channel, where a D_s^+ signal has been reported in other experiments [13]. The small excess of events near to the D_s^+ mass is barely significant and disappears if the vertex separation cut is increased. Figure 4 shows the $\phi\pi^+\pi^+\pi^-$ mass distribution for $N_\sigma > 8$. Upper limits for the branching ratios are given in Tables 1 and 2. Our limit of 0.24 for the D_s^+ is lower than the measurements reported in Ref. [13].

4. EXTRACTION OF THE $D_s \rightarrow \phi\pi^+$ BRANCHING FRACTION

Measurements of the decay channels $D_s^+ \rightarrow \phi\pi^+$, $D^+ \rightarrow K^-\pi^+\pi^+$, and $D^+ \rightarrow \phi\pi^+$ allow us to extract the ratios

$$\frac{\sigma(D_s^+)\text{Br}(D_s^+ \rightarrow \phi\pi^+)}{\sigma(D^+)\text{Br}(D^+ \rightarrow K^-\pi^+\pi^+)} \quad \text{and} \quad \frac{\sigma(D_s^+)\text{Br}(D_s^+ \rightarrow \phi\pi^+)}{\sigma(D^+)\text{Br}(D^+ \rightarrow \phi\pi^+)}.$$

For the D^+ , the channel $D^+ \rightarrow K^-\pi^+\pi^+$ yields the largest number of events. However, the second ratio is less sensitive to systematic uncertainties since it is derived using the same $\phi\pi^+$ channel for both D_s^+ and D^+ .

Using the branching fractions

$$\text{Br}(D^+ \rightarrow K^-\pi^+\pi^+) = (7.8 \pm 1.1)\% \quad [9],$$

$$\text{Br}(D^+ \rightarrow \phi\pi^+) = (0.57 \pm 0.14)\% \quad [9],$$

$$\text{Br}(\phi \rightarrow K^+K^-) = 0.495,$$

we derived the values $(2.13 \pm 0.56)\%$ and $(1.49 \pm 0.57)\%$ respectively for the ratio $\sigma(D_s^+) \cdot \text{Br}(D_s \rightarrow \phi\pi^+)/\sigma(D^+)$. The quoted uncertainties are a quadratic combination of statistics and systematics for D^+ channels. The common uncertainties from the

D_s^+ channel are not included, so that we can verify the compatibility of the two values. Combining them and including the statistical uncertainty coming from the D_s^+ we obtain

$$\frac{\sigma(D_s^+)}{\sigma(D^+)} \text{Br}(D_s^+ \rightarrow \phi\pi^+) = (1.81 \pm 0.63)\% \quad .$$

To deduce, from this measurement, a value for the D_s^+ branching fraction into $\phi\pi^+$, we need a model that predicts $\sigma(D_s^+)/\sigma(D^+)$. We have used the Lund model to hadronize the final-state partons, produced in a photon–nucleon interaction according to the dual parton model [14].

The most important parameters for this prediction in the Lund model are taken as follows: abundance of strange quarks relative to up quarks $p(s)/p(u) = 0.30$; relative production of D^* , $D^*/(D^*+D) = 0.75$ (from the spin counting rule); $\text{Br}(D^{*+} \rightarrow D^+X) = 50\%$. The corresponding experimental values are respectively 0.30 ± 0.07 [15], 0.80 ± 0.05 [16], and $(51 \pm 8)\%$ [9].

From the simulation we obtain the cross-section ratio

$$\sigma(D_s^+)/\sigma(D^+) = 0.38 \pm 0.15 \quad .$$

The uncertainty comes from the errors on the three Lund-model parameters. Using this ratio, we get:

$$\text{Br}(D_s^+ \rightarrow \phi\pi^+) = 4.8 \pm 1.7 \pm 1.9 \quad ,$$

where the first error is experimental and the second comes from the uncertainty on the cross-section ratio.

5. CONCLUSIONS

Several Cabibbo-favoured D_s^+ and Cabibbo-suppressed D^+ decays have been investigated. The data confirm that the ‘colour suppression mechanism’ does not operate. Our measurements on D_s^+ decays agree with theoretical expectations, except for the $\phi\pi^+\pi^0$ mode, for which the branching fraction is less than 2.6 times that of the $\phi\pi^+$ mode, well below the theoretical prediction.

By measuring the relative production rates of D^+ and D_s^+ and using a specific model, we extract a value for the branching fraction of the D_s^+ into $\phi\pi^+$.

REFERENCES

- [1] P. Astbury et al., *Phys. Lett.* **152B** (1985) 419.
- [2] R. Barate et al., *Nucl. Instrum. Methods* **A235** (1985) 235.
G. Barber et al., *Nucl. Instrum. Methods* **A253** (1987) 530.
M. Primout, Thèse d'État, CEN-Saclay, 1987.
- [3] R.W. Forty (NA14/2 Collab.), *Proc. 24th Int. Conf. on High Energy Physics, Munich, 1988* (Springer, Berlin, 1989), p. 668.
C. Magneville (NA14/2 Collab.), *Proc. 23rd Rencontres de Moriond, Les Arcs, 1988, 'Current Issues in Hadron Physics'* (Éd. Frontières, Gif-sur-Yvette, 1988), p. 455;
P. Roudeau (NA14/2 Collab.), *Proc. 23rd Rencontres de Moriond, Les Arcs 1988, 'Current Issues in Hadron Physics'* (Éd. Frontières, Gif-sur-Yvette, 1988), p. 499.
M.P. Alvarez et al. (NA14/2 Collab.), preprint CERN-EP/90-26 (1990), submitted to *Z. Phys. C*.
- [4] M.P. Alvarez et al. (NA14/2 Collab.), preprint CERN-EP/88-148 (1988).
- [5] N. Cabibbo and L. Maiani, *Phys. Lett.* **73B** (1978) 418.
A.J. Buras, J.-M. Gerard and R. Rückl, *Nucl. Phys.* **B268** (1986) 16.
B.Yu. Blok and M.A. Shifman, *Sov. J. Nucl. Phys.* **45** (1987) 522.
- [6] C. Magneville, Thèse d'État, CEN-Saclay, 1987.
- [7] R.W. Forty, PhD thesis, Imperial College London, 1988.
- [8] P. Druet, Thèse d'Université, Orsay, 1988.
- [9] G.P. Yost et al., Particle Data Group, *Phys. Lett.* **B204** (1988) 1.
- [10] J. Adler et al., *Phys. Rev. Lett.* **60** (1988) 1989.
- [11] M. Bauer, B. Stech and M. Wirbel, *Z. Phys.* **C34** (1987) 103.
- [12] J.C. Anjos et al., *Phys. Lett.* **B223** (1989) 267.
- [13] J.C. Anjos et al., *Phys. Rev. Lett.* **60** (1988) 897.
M.S. Witherell, *Proc. 24th Int. Conf. on High Energy Physics, Munich, 1988* (Springer, Berlin, 1989), p. 478.
- [14] A. Capella and J. Tran Thanh Van, *Phys. Lett.* **93B** (1980) 146.
P. Roudeau, *Nucl. Phys. B (Proc. Suppl.)* **1B** (1988) 33.
- [15] A. Dresler, *Proc. 24th Int. Conf. on High Energy Physics, Munich, 1988* (Springer, Berlin, 1989), p. 1024.
- [16] M. Derrick, *Proc. 24th Int. Conf. on High Energy Physics, Munich, 1988* (Springer, Berlin, 1989), p. 895.

Table 1
Results for D^+ (limits are given at 90% CL).

Decay channel	Branching ratio relative to $D^+ \rightarrow K^- \pi^+ \pi^+$	Branching fraction [Assuming $BR(D^+ \rightarrow K^- \pi^+ \pi^+) = 7.8\%$] (%)
$D^+ \rightarrow \phi \pi^+$	$0.098 \pm 0.032 \pm 0.014$	$0.76 \pm 0.25 \pm 0.11$
$D^+ \rightarrow \bar{K}^{*0} K^+$	< 0.11	< 0.86
$D^+ \rightarrow \phi \pi^+ \pi^0$	< 0.58	< 4.5
$D^+ \rightarrow \phi \pi^+ \pi^+ \pi^-$	< 0.031	< 0.24

Table 2
Results for D_s^+ (limits are given at 90% CL).

Decay channel	Branching ratio relative to $D_s^+ \rightarrow \phi \pi^+$
$D_s^+ \rightarrow \bar{K}^{*0} K^+$	$0.85 \pm 0.34 \pm 0.20$
$D_s^+ \rightarrow \phi \pi^+ \pi^0$	< 2.6
$D_s^+ \rightarrow \phi \pi^+ \pi^+ \pi^-$	< 0.24

Figure captions

- Fig. 1 $\phi\pi^+$ effective mass distribution (using a vertex separation cut: $\Delta x > 2$ mm).
- Fig. 2 $\bar{K}^{*0}K^+$ effective mass distribution (using a vertex separation cut: $N_\sigma > 3.5$).
- Fig. 3 $\phi\pi^+\pi^0$ effective mass distribution (using a vertex separation cut: $N_\sigma > 8$).
- Fig. 4 $\phi\pi^+\pi^+\pi^-$ effective mass distribution (using a vertex separation cut: $N_\sigma > 8$).

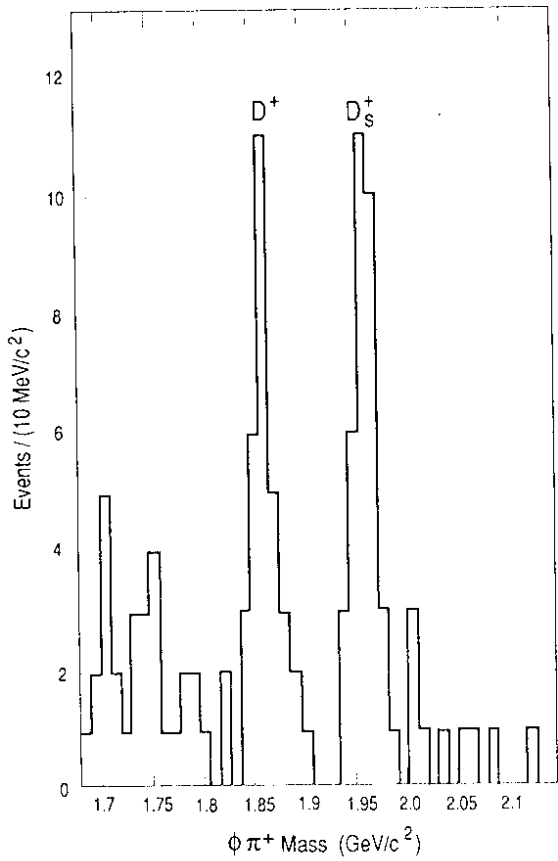


Fig. 1

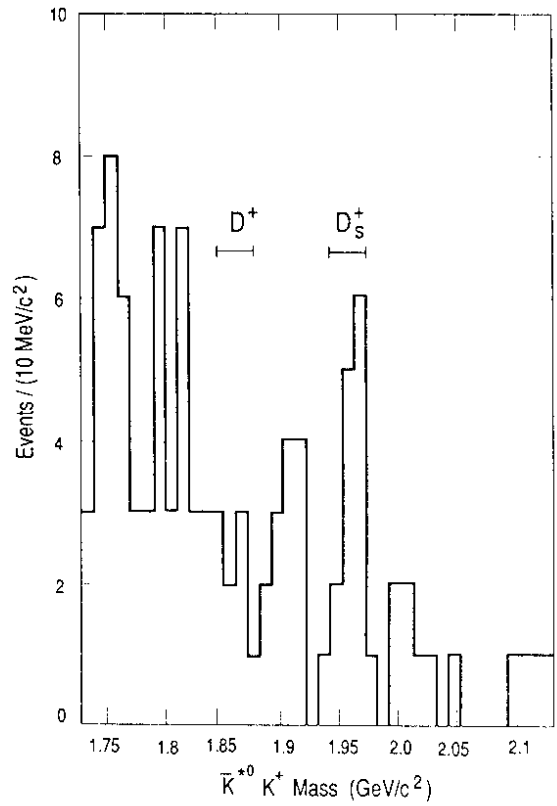


Fig. 2

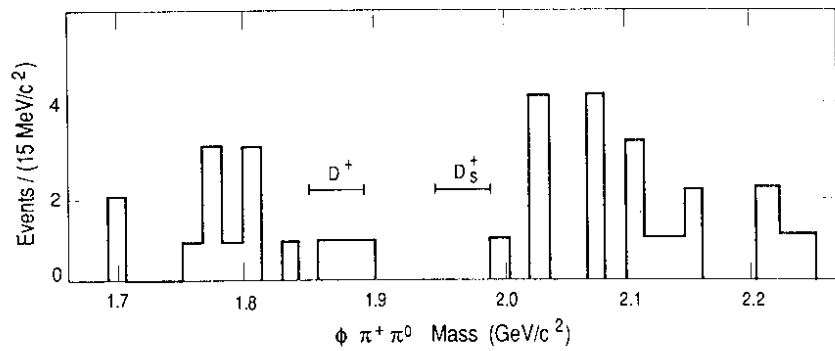


Fig. 3

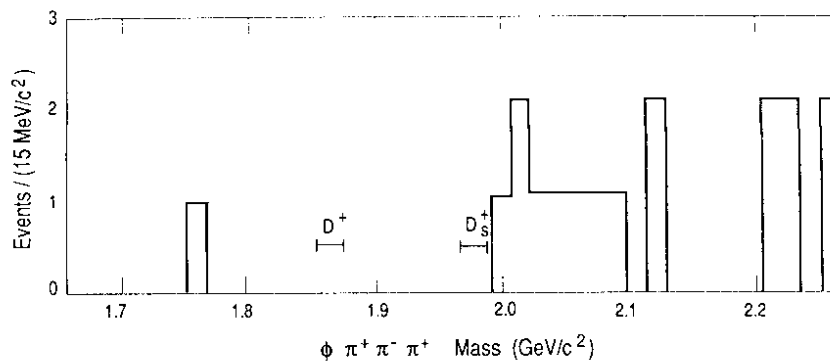


Fig. 4